

Chapter 10

Synthesis and Characterization of Polyhedral Oligomeric Silsesquioxane-Core Star Polystyrene via Nitroxide-Mediated Polymerization

David Glé,¹ Trang N. T. Phan,^{*,1} Valérie Monier,² Laurence Charles,¹ Denis Bertin,¹ and Didier Gigmes^{*,1}

¹UMR-CNRS 7273, Institut de Chimie Radicalaire Fédération des Sciences Chimiques de Marseille, Aix-Marseille Universités, Service 542, Avenue Escadrille Normandie Niemen, 13397 Marseille Cedex 20, France

²Spectropole, Fédération des Sciences Chimiques de Marseille, Aix-Marseille Universités, Service 542, Avenue Escadrille Normandie Niemen, 13397 Marseille Cedex 20, France

*E-mails: trang.phan@univ-amu.fr, didier.gigmes@univ-amu.fr.

Phone: 33 (0)491 288 097. Fax: 33 (0)491 288 758.

Multifunctional NMP initiator with a core of cubic silsesquioxane (POSS) was synthesized starting from the coupling of Octa(3-aminopropyl)octasilsesquioxane with 2-Methyl-2-[N-tert-butyl-N-(1-diethoxyphosphoryl)-2,2-dimethylpropyl]aminoxyl-N propionyloxysuccinimide. The obtained POSS-based multialkoxamine was then used as NMP initiator for the polymerization of styrene leading to the formation of star polystyrenes of narrow dispersity with a core consisting of dispersed nanosized hard particles. We demonstrated that stars with a predetermined molecular weight and a control of dispersity could be synthesized by simply controlling reaction parameters and restricting the monomer conversion typically below 30 - 35%. The precise structure of POSS based star polystyrenes was analyzed by the characterization of the individual arms obtained after etching the Si-O-Si bonds of the core. The influence of POSS core

on the glass transition temperature of nanocomposites was investigated and compared to that of their cleaved products using differential scanning calorimetry.

Introduction

Star polymers are a class of branched polymers consisting of at least three linear polymeric chains radiating from one single multifunctional branching point, usually called the core or the central nodule (1). They differ from the linear analogues of identical molecular weight not only on the compact structure but also on the multiple functionality that is useful in some of their applications. Synthesis of star polymers is most often accomplished by living ionic polymerization (2, 3) or controlled/living radical polymerization (4–8). There are essentially two strategies to synthesize star polymers: the “arm-first” method (9, 10), which cross-links preformed macroinitiators using divinyl molecules and the “core-first” method (4, 5), which uses an active multifunctional core to initiate the polymerization of monomers. A variation of “arm-first” technique, the “coupling-onto” method, involves attaching of preformed arms onto a multifunctional core (11, 12). Although the “arm-first” approach is the easiest way to synthesize star polymer containing multiple arms and functionalities, they unfortunately lead to star polymers having statistical distribution of the number of arms and a relatively broad molecular weight distribution. The final product is also contaminated by the residual unreacted starting linear polymers. These problems come from the difficulty of achieving 100 % linkage of the chains to the core caused by increasing steric hindrance of the already attached long chains.

Recently, Matyjaszewski et al. (13, 14) developed an other variation of “arm-first” method which consists in a copolymerization of linear macromers with a divinyl cross-linker using low molar mass initiators. With this method, the number of initiating sites and number of arms per star molecule are independently controlled. Thus, the star-star coupling reactions could be minimized by lowering the molar ratio of initiator to macromer, providing star polymers with low-polydispersities. As for most of the variant of “arm-first” method, the contamination of the final product by the residual unreacted macromer is inevitable unless macromer conversion reaches the high values (> 95%), but that requires often a long reaction time (about 24h or even several days for some macromers).

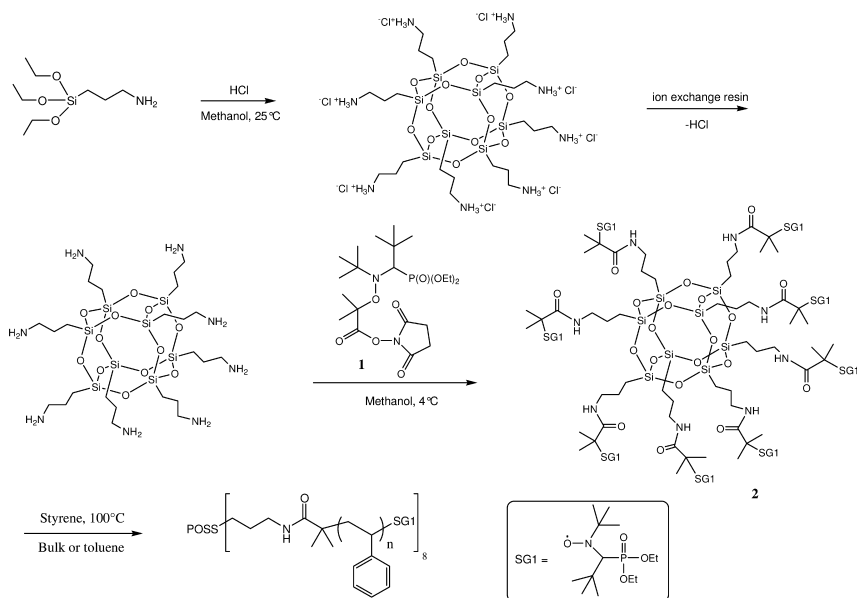
Well-defined star polymers offer many interesting properties such as lower melting points, lower solution viscosities, more processable and superior mechanical properties compared to the corresponding linear polymer of similar molecular weight. Their synthesis requires the use of initiator with precise functionality. “Core-first” approach has been proved to be efficient to prepare a series of star polymers with precise arm numbers and lengths via controlled radical polymerization techniques such as nitroxide mediated polymerization (NMP) (15), atom transfer radical polymerization (ATRP) (4, 5), and reversible addition-fragmentation chain transfer polymerization (RAFT) (8) as well ring opening polymerization (ROP) (16–18). The synthesis of star polymers with 3-,

4-, 6-, 7-, 8-, and even 12-arms has been described by several research groups using either organic or inorganic initiators. The synthesis of star polymers initiated by inorganic cores would have the advantages of combining the unique characteristics of both the organic/inorganic materials and star-like polymers.

Polyhedral oligomeric silsesquioxanes (POSS) reagents combine unique hybrid (inorganic–organic) chemical compositions with nano-sized cage structures that have dimensions comparable with those of most polymer segments. A typical POSS molecule possesses the structure of cube-octameric frameworks represented by the formula $(R_8Si_8O_{12})$ with an inorganic silica-like core (Si_8O_{12}) surrounded by eight organic corner groups, which can be functionalized by a variety of organic reactive groups. POSS in polymer matrix has been found various applications in the areas such as liquid crystals (19), nanocomposites (20), photo-resists in lithographic technologies (21), based on their high thermal stability and oxidation resistance properties (22–24). A numbers of reports have been published on organic/inorganic hybrids containing pendant POSS (25–27). However, little work reported on the synthesis of well-defined hybrid star-like polymers by controlled radical polymerization using POSS as core. The first report on the used of POSS-based octafunctional ATRP initiator for the polymerization of methyl methacrylate was published by Laine et al (28). The resulting hybrid star-like polymers had polydispersity increasing as the polymerization progressed, additionally; the star-star coupling was observed for conversion as low as 20%, indicating a poor control on the synthesis. Recently, He et al. (29) and Liu et al. (30) reported the synthesis of POSS-(Br)₈ initiators and their use as multifunctional initiator for the ATRP of methyl methacrylate in acetonitrile/water mixture and that of styrene in anisole. In both reports, the authors obtained hybrid star polymers with low polydispersity (1.17 and 1.08, respectively). However, to obtain well-defined hybrid star polymers, these authors had stopped polymerization at quite low monomer conversion about 23%. Compared to ATRP techniques, there are relatively few studies that have exploited NMP for the synthesis of POSS-core star polymers. Indeed, we are only aware of one report in which Kuo et al. (31) described the synthesis of an octa-N-alkoxyamine POSS through the hydrosilylation of octakis(dimethylsiloxy) silsesquioxane (with 1-(2-(allyloxy)-1-phenylethoxy)-2,2,6,6-tetramethylpiperidine (allyl-TEMPO) in the presence of Karstedt's agent. This multifunctional initiator was further used for the synthesis of POSS based star polystyrene as well as several diblock copolymers. Bulk styrene polymerization was achieved at 80% monomer conversion after 17h at 120°C for a target molecular weight of 80000 g/mol. Interestingly, these authors didn't observe any star coupling reactions for a monomer conversion as high as 63% while other studies demonstrated that inter or intra-star coupling reactions appear once monomer conversion exceeds 25% (4, 28, 30). The occurrence of star coupling reaction is usually evidenced by detection of shoulder in the chromatographic traces at the high molecular weigh region.

With the growing interest of POSS based materials in various applications and the desire to investigate different convenient alternative of the NMP process in such system for successful synthesis of POSS based star polymers, we describe, in this paper, the synthesis of star polystyrene from a cubic silsesquioxane NMP

initiator using the “core-first” method. The strategy for the synthesis of hybrid star polystyrene with POSS core consist of three main steps depicted in Scheme 1. i) synthesis of octa(3-ammoniumpropyl)octasilsesquioxane octachloride [POSS-(NH₃⁺Cl)₈]; ii) neutralization of POSS-(NH₃⁺Cl)₈ followed immediately by its coupling with an alkoxyamine bearing a *N*-succinimidyl (NHS) ester group **1** to prepare the corresponding POSS-alkoxyamine initiator **2**; iii) solution or bulk polymerization of styrene by NMP using POSS-alkoxyamine **2** as initiator.



Scheme 1. Schematic illustration for the preparation of Octa(3-ammoniumpropyl)octasilsesquioxane Octachloride [POSS-(NH₃⁺Cl)₈] and POSS-based octafunctional NMP initiator [POSS-(SG1)₈].

Experimental Section

Materials

MAMA-SG1 (Blocbuilder MA[™] >99%), (scheme 1) derived was kindly provided by Arkema (France). 3-aminopropyltrimethoxysilane (97%), styrene (99%), dicyclohexylcarbodiimide (99%), and *N*-hydroxysuccinimide (98%) were purchased from Aldrich and used as received. All solvents and other chemicals were of reagent-grade quality and were obtained commercially and used without further purification.

Characterization

All ^1H , ^{31}P and ^{29}Si NMR were run either in DMSO-d_6 or in CDCl_3 and recorded in a Bruker AV400 MHz spectrometer. Number-average molecular weights (M_n) and molecular weights distribution (M_w/M_n) of resulting hybrid star polystyrene were determined by size exclusion chromatography operated at 30°C . The chromatographic device was equipped with a Waters 515 liquid chromatograph pump, a guard column and two Nucleogel (HR4 and HR5) columns in series. Detection systems were a differential refractive index detector (Waters Model 410) and a ultra-violet (UV) detector (Waters Model 468). The mobile phase was tetrahydrofuran with a flow rate of 1.0 mL min^{-1} . Calibration based on polystyrene standards from Polymer Laboratories (molecular weight range: 580 - 377 400 g mol^{-1}) was applied for the determination of molecular weights of star polymers.

Electrospray ionization mass spectroscopy (ESI-MS) experiments were performed with a QStar Elite mass spectrometer (Applied Biosystems SCIEX, Concord, ON, Canada) equipped with an electrospray ionization source operated in the positive ion mode. The capillary voltage was set at 5500 V and the cone voltage at 20 V. In this hybrid instrument, ions were measured using an orthogonal acceleration time-of-flight (oa-TOF) mass analyzer. Nitrogen was used as the nebulizing gas (10 psi) and the curtain gas (20 psi). POSS samples were dissolved in methanol at a concentration of 5 mg/mL ; this solution was then diluted in 1:10 volume ratio with a acidified methanol (0.5 % formic acid). The sample solution was then infused into the electrospray interface by a syringe pump at a flow rate of 5 $\mu\text{L/min}$.

The Differential Scanning Calorimetry (DSC) studies were carried out using a TA Instruments 2920 Modulated DSC. Typical sample masses for modulated DSC were 3-5 mg. The samples were first heated from room temperature to 130°C at a heating rate of 5°C/min under nitrogen atmosphere, followed by cooling to 40°C at a cooling rate of 5°C/min after stopping at 130°C for 5 min to erase any prior thermal history. Finally, samples were analyzed by subsequent heating to 130°C under modulation mode. The modulation conditions include period of 60 sec, modulation amplitudes of $\pm 0.8^\circ\text{C}$, and a scanning rate of 3°C/min . The glass transition temperature (T_g) was determined on the transition of the final heating process and was chosen at the 50% change of the heat capacity that is close to the point of inflection.

Octakis(3-ammoniumpropyl)octasilsesquioxane Octachloride (POSS- NH_3^+Cl^-)

POSS- NH_3^+Cl^- was prepared in a round bottom two neck-flask equipped with a magnetic stirrer and nitrogen purge. First, 400 mL of methanol was placed in the flask, and then 50 mL (0.213 mol) of 3-aminopropyltrimethoxysilane was introduced dropwise. After the complete addition of silane, 67.5 mL of concentrated hydrochloric acid (36.5 wt%, 12 M) was poured quickly and the flask was closed when the fume production stopped (about 5 minutes). The reaction mixture was then stirred under nitrogen at room temperature for one

week. POSS- NH_3^+Cl^- precipitated as a white powder and was formed after 5 days. The crude product obtained after filtration, washing with cold dry methanol, and drying was spectroscopically pure in 30% yield (9.6 g). Recrystallization from hot dry methanol afforded POSS- NH_3^+Cl^- (4.29 g, 3.66 mmol, 6.88%) as a white solid. ^{29}Si NMR (DMSO- d_6 , δ , ppm): -66.44. ^1H NMR (DMSO- d_6 , δ , ppm): 8.23 (s, 24H, NH_3^+Cl^-), 2.76 (t, 16H, $\text{NH}_3^+-\text{CH}_2-\text{CH}_2$), 1.71 (m, 16H, $\text{CH}_2-\text{CH}_2-\text{Si}$), 0.72 (t, 16H, CH_2-Si).

Octakis(2-Methyl-2-(N-tert-butyl-N-(1-diethoxyphosphoryl)-2,2-dimethylpropyl)aminoxy)-N-propyl propionamide)octasilsesquioxane (POSS-MAMA-SG1, 2)

Amberlite IRA-400 ion-exchange resin (30 g) was prepared by successive washing with water (4 x 150 mL), 1M NaOH (3x150 mL), water (6x150 mL), and methanol (6x150 mL), which was the elution solvent; the resin was suspended in eluent and chilled (-10 °C, 2 h) before use. Half of the resin beads were loaded onto a column (3.5 cm outside diameter), and the other half were used to dissolve a suspension of neutralized POSS- NH_3^+Cl^- (1.43 g, 1.22 mmol) in the minimum amount of eluent below 0°C. Elution across the column produced a methanol solution of neutralized POSS- NH_2 . Immediately, NHS-MAMA-SG1 **1**, previously prepared in a straightforward manner from the commercially available MAMA-SG1 according to the literature method (32) (6.46g, 9.76 mmol, 8 equiv) was added to a solution of neutralized POSS- NH_2 , and the resulting mixture was kept under magnetic stirring at 4°C during 2h. Methanol was then evaporated under reduced pressure and the product was precipitated in cold pentane. The obtained solid was respectively washed with distilled water to remove N-hydroxysuccinimide and with diethyl ether to remove the unreacted NHS-MAMA-SG1. POSS-MAMA-SG1 **2** was obtained as a white powder after drying under vacuum at room temperature. Yield: 50%. ^{31}P NMR (CDCl_3 , δ , ppm): 27.51. ^{29}Si NMR (DMSO- d_6 , δ , ppm): -66.22. ^1H NMR (CDCl_3 , δ , ppm): 5.58 (broad peak, 8H, $\text{NH}-\text{C}=\text{O}$), 3.95 – 4.46 (m, 32H, $\text{CH}_3-\text{CH}_2-\text{O}-\text{P}$), 3.30 (d, $J(\text{H},\text{P}) = 27$ Hz, 8H, $\text{N}-\text{CH}-\text{P}$), 2.74 -3.08 (m, 16H, $\text{CH}_2-\text{NH}-\text{C}=\text{O}$), 1.48 – 2.02 (m, 64H, $\text{CH}_3-\text{C}-\text{CO}$ and $\text{CH}_2-\text{CH}_2-\text{Si}$), 0.98 –1.45 (m, 192H, CH_3 of *tert*-butyl and $\text{CH}_3-\text{CH}_2-\text{O}-\text{P}$), 0.67 (t, 16H, CH_2-Si).

Synthesis of Star Polystyrene Using POSS-MAMA-SG1 as NMP Initiator

Styrene (3.0g, 2.86×10^{-2} mols), POSS-MAMA-SG1 (127mg, 2.78×10^{-5} mols), and toluene (2g) were weighted and mixed to generate a solution that contained 60 wt % of monomer. This solution was placed in a three-neck flask equipped with a reflux condenser and a magnetic stir bar. The mixture was purged for 20 min with argon at room temperature to remove oxygen. In kinetic studies, samples were collected from the reaction mixture at given time intervals by a syringe through a septum. Styrene conversion was determined by ^1H NMR in CDCl_3 . Average molar mass and molecular weight distribution were determined by size exclusion chromatography (SEC). The polymerization was stopped by

quenching the reactor in an ice bath. The polymer was purified by precipitation in ethanol, filtered to remove the volatiles and dried under high vacuum at room temperature to a constant weight.

Cleavage of POSS-PS Star Polymer

50 mg POSS-PS star polymer was dissolved in 2 mL of THF in a polypropylene tube, and then 40 μ L HF solution (40 wt %) was added to the solution (**Caution : Hydrofluoric acid is extremely corrosive**). After stirring at 50 $^{\circ}$ C for 15h and then removing all the solvents by vacuum, the residues were dissolved in 0.5 mL CH_2Cl_2 and precipitated into an excess of methanol. The solid was collected by filtration and dried in a vacuum at room temperature before analyze by SEC.

Results and Discussion

NMP Initiator Syntheses

POSS- $(\text{NH}_3^+\text{Cl}^-)_8$ was prepared according to the reported method (33, 34). The produced POSS- $(\text{NH}_3^+\text{Cl}^-)_8$ had appearance of a white solid and was spectroscopically pure in 30 % yield; as might be expected for an octa-(ammonium chloride) salt, it was highly hydroscopic. Neutralization of POSS- $(\text{NH}_3^+\text{Cl}^-)_8$ was accomplished by eluting it as a methanol solution across a column of Amberlite IRA-400 resin according to the reported method (34, 35). The preparation of NHS-activated ester alkoxyamine was previously reported by our group (32) in which we demonstrated the effectiveness of this alkoxyamine in the polymerization of styrene and *n*-butyl acrylate and especially its potential in the synthesis of hydroxyl-functionalized polystyrene and OH-functional alkoxyamine. This latter was easily obtained in a high yield by reaction of alkoxyamine **1** and ethanolamine. Thus, following this strategy, we synthesized POSS-alkoxyamine **2**. Typically, to a methanol solution of the freshly prepared POSS- $(\text{NH}_2)_8$ was added the NHS-activated ester alkoxyamine **1**, and the resulting mixture was held at 0 $^{\circ}$ C for 2 hours. After removal of the solvent under reduced pressure, the POSS-alkoxyamine **2** was isolated as a white powder, easy to store and handle after precipitation in pentane. Two experiments were carried out, the first one with an equimolar ratio of amine group and alkoxyamine **1** and the second one with a molar ratio of alkoxyamine **1** to amine group equals to 1.5. The ^{31}P NMR analysis of the crude products after removal of methanol solvent allows the determination of the reaction yield (Figure 1). Typically, by comparison of the integral value of the peak at $\delta = 27.5$ ppm corresponding to the POSS-MAMA-SG1 alkoxyamine **2** with the one of the peak at $\delta = 25$ ppm corresponding to the starting alkoxyamine **1**, the reaction yield for the two experiments was respectively 83 mol % and 100 mol %. The unreacted NHS-MAMA-SG1 was removed from POSS-MAMA-SG1 alkoxyamine **2** by

rinsing out the crude product with cold diethyl ether. This treatment was only efficient for the purification of crude product resulting from the experiment with an equimolar of POSS amine groups and alkoxyamine **1** as shown in the ^{31}P NMR spectra of the resulting POSS-MAMA-SG1 alkoxyamine (Figure 2). However, it was more difficult to remove completely the excess alkoxyamine **1** in the crude product resulting from the experiment with an excess of alkoxyamine **1** compared to POSS amine groups. In such case, the work up of the reaction mixture was accompanied with an important loss of the formed POSS-MAMASG1 alkoxyamine **2**. This is probably due to a similar affinity of the POSS that has all the available sites reacted with MAMA-SG1 and the excess alkoxyamine **1** towards diethyl ether.

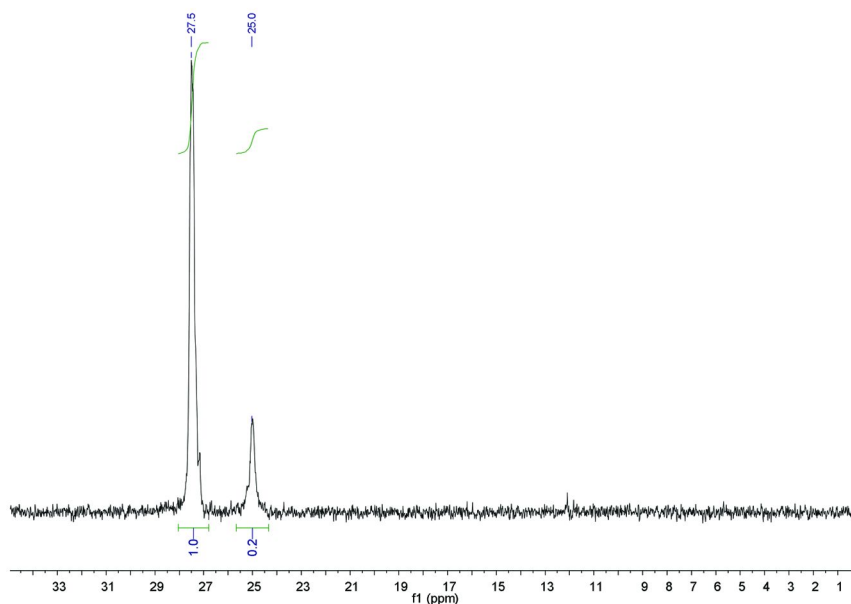


*Figure 1. ^{31}P NMR spectrum from the crude product of POSS-MAMA-SG1 alkoxyamine **2**, product obtained in the experiments with an equimolar ratio of amine group and alkoxyamine **1**, in CDCl_3 .*

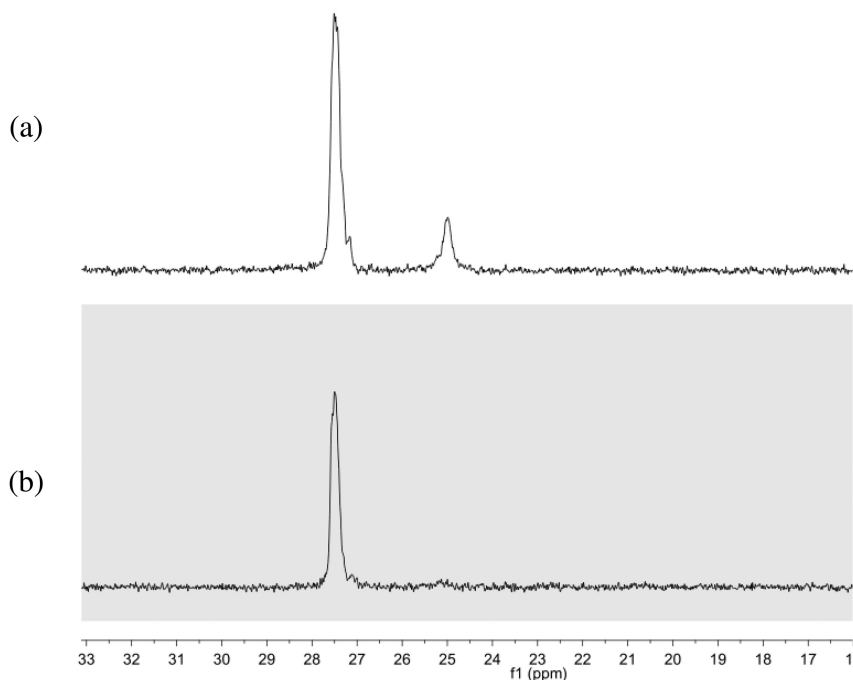


*Figure 2. ^{31}P NMR spectra of POSS-MAMA-SG1 alkoxyamine **2** (a) before and (b) after washing with diethyl ether, products resulting from the experiment working with an equimolar ratio of amine group and alkoxyamine **1**, in CDCl_3 .*

In addition to NMR analysis, ESI-MS was used to characterize the functionality of POSS based alkoxyamines. The ESI mass spectrum of POSS-MAMA-SG1, product resulting from experiment 1 (Figure 3), indicated the absence of a peak corresponding to the unreacted NHS-MAMA-SG1 but also the presence of different POSS based alkoxyamine species with 3 to 6 initiating sites (MAMA-SG1) per POSS molecule. As expected, the ESI mass spectrum of POSS-MAMA-SG1 (not shown here), product resulting from experiment 2, shown the peak corresponding to the unreacted NHS-MAMA-SG1 ($[\text{M} + \text{H}]^+$ at m/z 479.2) that could not be completely eliminated from the crude product as well as the presence of several peaks corresponding to POSS based alkoxyamine with 5, 6, 7 and 8 initiating sites. By combination of these different characterizations, we denote afterwards, POSS-MAMA-SG1(a) as the “pure” alkoxyamine **2** having about 5 - 6 initiating sites (NMR value) per POSS molecule and POSS-MAMA-SG1(b) as the sample containing both NHS-MAMA-SG1 and 7 - 8 initiating sites (NMR value) per POSS molecule.

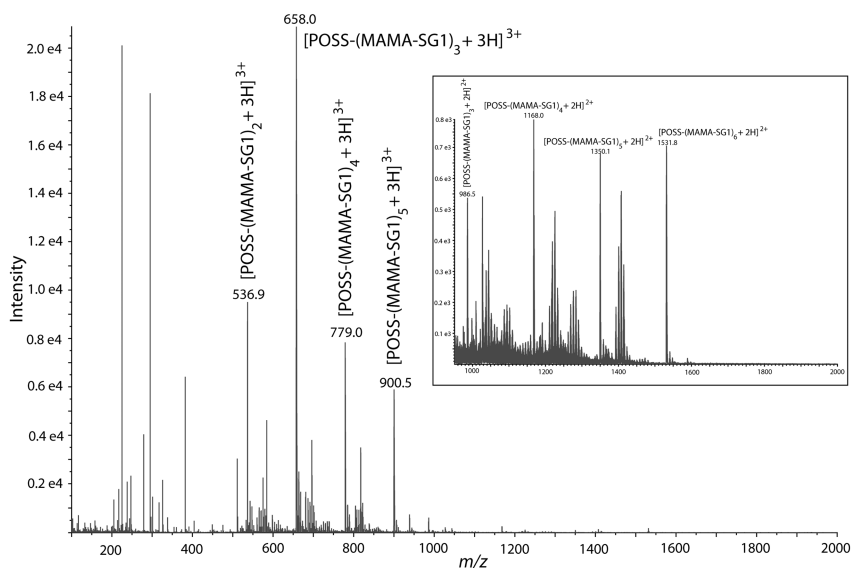


Figure 3. ESI mass spectrum of POSS-based alkoxyamine prepared in the experiment working with an equimolar ratio of amine group and alkoxyamine 1. The spectrum indicates the formation of POSS-(MAMA-SG1)_n, with n ranging from 2 to 6. Inset : zoom of the mass spectrum in the m/z range 900-2000.

Synthesis of Star PS

The advent of controlled radical polymerization techniques, such as NMP, ATRP, and RAFT, has rendered the preparation of well-defined star polymers much easier, starting from proper multifunctional initiators with known number of initiating sites. Most star polymers with varying number of arms have been prepared via ATRP “grafting-from” strategy (4–6, 36). Starting from POSS-based octafunctional ATRP initiator, organic/inorganic nanocomposite star polymers have been recently prepared by Laine et al. (28), He et al. (29), and Liu et al (30).

The obtained POSS-MAMA-SG1 alkoxyamine **2** was then used as multifunctional initiator for the NMP of styrene. Five different polymerizations of styrene were carried out either in bulk or in solution using toluene or ethyl benzene as solvent. The reaction conditions are detailed in Table 1. Whatever the targeted molecular weight and polymerization process, the kinetic curves relative to $\ln([M]_0/[M])$ versus time was of first order with respect to monomer (Figure 4), indicating a constant concentration of active species throughout the reaction. As expected, the polymerization rate was significantly higher in bulk than in solution polymerization at the same polymerization temperature (Figure 4, entries (1) and (2)) as well as when the initiator concentration is high (Figure 4, entries (2) and (3)). Indeed, polymerization rate is proportional to monomer and initiator concentration, and these concentrations were lower in the solution polymerization than in the bulk one.

Table 1. Reaction conditions tested for the synthesis of star PS using POSS-MAMA-SG1 alkoxyamine 2 as initiator

Entry	Styrene g (mol)	POSS- MAMA-SG1 mg (mol)	Solvent	target M_n^c (g.mol ⁻¹)	T (°C)	over- all time (min)
(1) ^a	3.00 (2.86 x10 ⁻²)	127 (2.78 x10 ⁻⁵)	Toluene	110 000	100	420
(2) ^a	3.00 (2.86 x10 ⁻²)	127 (2.78 x10 ⁻⁵)	/	110 000	100	210
(3) ^a	3.00 (2.86 x10 ⁻²)	71 (1.57 x10 ⁻⁵)	/	190 000	100	210
(4) ^a	3.00 (2.86 x10 ⁻²)	127 (2.78 x10 ⁻⁵)	Ethyl- benzene	110 000	120	180
(5) ^b	3.00 (2.86 x10 ⁻²)	127 (2.78 x10 ⁻⁵)	Toluene	110 000	100	420

^a Studies (1), (2) and (3) were performed using POSS-MAMA-SG1(a) resulting from the experiment with an equimolar of POSS amine groups and alkoxyamine 1. ^b Study (5) was performed using POSS-MAMA-SG1(b) resulting from the experiment with an excess of alkoxyamine 1 compared to POSS amine groups, it means that the product contains both mono and multifunctional initiators. ^c Expected star-polymer molar mass at 100% conversion. Monomer concentration in solvent was fixed at 60 wt % for all solution polymerisations.

Control over the growth of polymer chains was furthermore evidenced by the linear evolution of molecular weight with conversion as well as a low polydispersity of 1.14 at monomer conversion of 40% (Figure 5). Experiments (1) and (2) have the same theoretical line because they only differ on the polymerization conditions (bulk or solution polymerization), it may only affect the reaction kinetic. As it can be seen, the experimental molecular weights data corresponding to experiments (1), (2) and (3) are slightly below the theoretical ones which were calculated from the relation $M_{n(th)} = ([M]/[I]_0 \times MW_{monomer}) + MW_{initiator}$. It has been pointed out that the radius of gyration of a star molecule is lower than that of a linear molecule with the same molecular weight due to the packing of the chains attached to the same core. Therefore, the hydrodynamic properties are affected, and SEC analyses based on linear polystyrene standards give molecular weights lower than expected, causing the experimental data to shift to the region below the theoretical line.

There is not significant increase of polymer dispersity with monomer conversion in the experiments (2) and (3) which only differ to each other on the initiator concentration. Dispersities of 1.14 and 1.17 are obtained for polymers generated from entry (2) and (3) respectively. The obtained polymers with broader M_n distribution are usually expected when initiator concentrations is increased as noted by Laine et al. (28) in the ATRP of methyl methacrylate using POSS based initiator. Indeed, the increase of catalyst and initiator concentrations engenders radicals with longer average lifetime and a higher concentration of active stars present in the reaction medium. In consequence, the occurrence of termination reactions increases and polymers with broader M_n distribution were obtained.

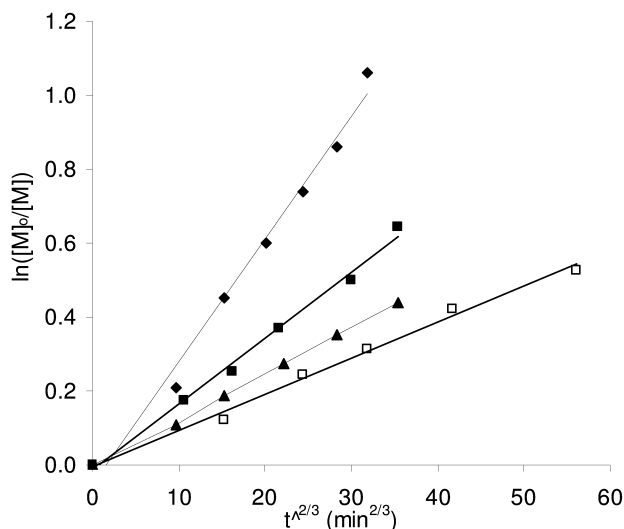


Figure 4. Semilogarithmic kinetics plot for the synthesis of star PS initiated by POSS-MAMA-SG1 under different polymerization conditions. \square : (1) solution polymerization in toluene at 100°C with $M_{n \text{ targeted}} = 110\,000 \text{ g.mol}^{-1}$, \blacksquare : (2) bulk polymerization at 100°C with $M_{n \text{ targeted}} = 110\,000 \text{ g.mol}^{-1}$; \blacktriangle : (3) bulk polymerization at 100°C with $M_{n \text{ targeted}} = 190\,000 \text{ g.mol}^{-1}$; \blacklozenge : (4) solution polymerization in ethylbenzene at 120°C with $M_{n \text{ targeted}} = 110\,000 \text{ g.mol}^{-1}$. For detailed conditions of these studies, refer to Table 1.

SEC traces shown in Figure 6 display unimodal and relatively symmetrical peaks for PS star polymers resulting from experiment (1). We note that chromatographic peaks became less and less symmetric with the increase of styrene conversion. Beyond 35% conversion, the base of peak trace becomes broader and a very slight shoulder appears in the high molar mass side of the SEC traces. This result can be attributed to the inter or intra-star coupling of the growing radicals due to irreversible termination reactions that are never totally negligible. Similar results have been already observed during the preparation of star polymers from POSS based or calixaren derivative octafunctional initiators (4, 28, 30). Nevertheless, the presence of higher molecular weight species derived from termination coupling observed in the chromatograms for experiments (1) (Figure 6), (2) and (3) (not shown here) were less pronounced than that reported in the literature at the same conversion.

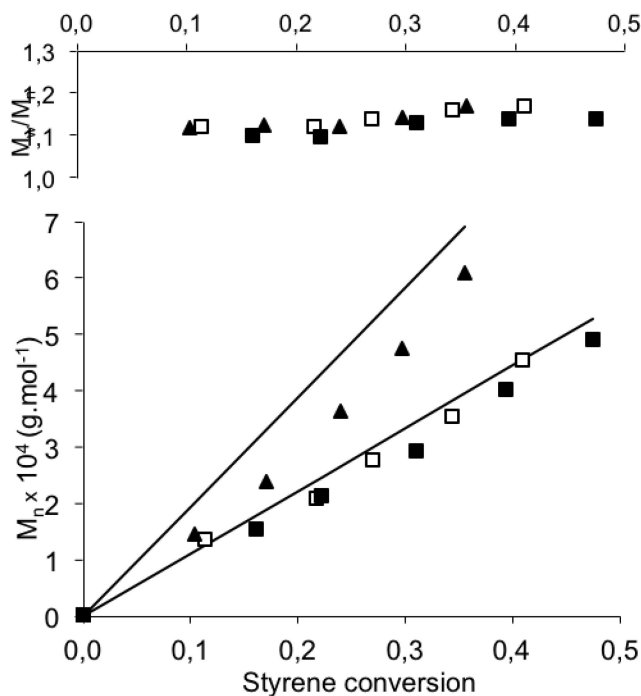


Figure 5. $M_{n(th)}$ (drawn line); M_n (symbols) and M_w/M_n versus conversion for star PS initiated by POSS-MAMA-SGI(a) under different polymerization conditions.

□: (1) solution polymerization in toluene at 100°C with $M_n \text{ targeted} = 110\,000 \text{ g.mol}^{-1}$;
 ■: (2) bulk polymerization at 100°C with $M_n \text{ targeted} = 110\,000 \text{ g.mol}^{-1}$;
 ▲: (3) bulk polymerization at 100°C with $M_n \text{ targeted} = 190\,000 \text{ g.mol}^{-1}$.

Experiments (1) and (4) were carried out in the same experimental conditions but at two different temperatures 100°C and 120°C. As expected, the polymerization rate was significantly higher at 120°C than at 100°C (Figure 4). Indeed, the cleavage rate constant k_d depends on the dissociation energy of the alkoxyamine bond and Arrhenius temperature while cross-combination constant k_c shows non-Arrhenius temperature dependencies (37). The polymerization proceeds to high conversion (65%) within three hours at 120°C. Figure 7 shows the chromatograms of polymers generated from polymerizations performed at 100°C and 120°C having similar molecular weight. As we can see, polymer formed from polymerization at 120°C exhibited broader distribution than that obtained by polymerization at 100°C, indicating that high temperature increases growing radical reactivity, thus favouring termination reactions and leads to more polydisperse materials. We also noted that the shoulder appearing in the high molar mass side of the SEC traces was visible since 60 min, corresponding to 32% monomer conversion, of polymerization carrying out at 120°C.

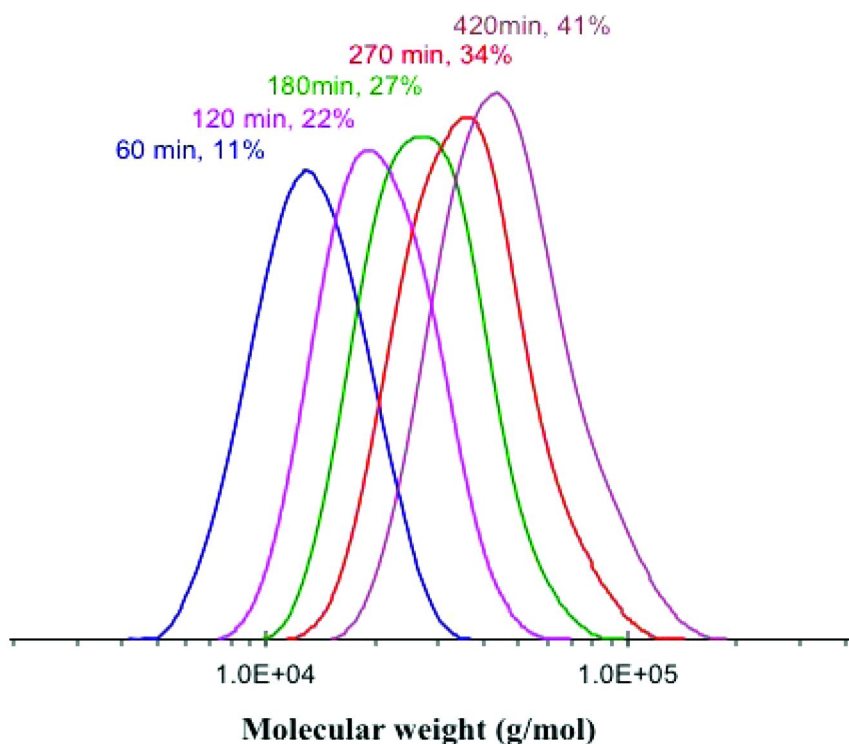


Figure 6. Evolution of SEC traces during synthesis of PS star polymer. Experimental conditions: $[\text{POSS-MAMA-SG1}]_0/[\text{styrene}]_0 = 1 : 1023$; in toluene at 100°C ; monomer concentration in solution = 60wt %; linear polystyrene standards were used for calibration of the THF SEC.

Through these different polymerizations, it seems that the optimum reaction conditions to obtain better control of the star architecture are low monomer conversion (not exceeding 30%) and low reaction temperature. These parameters are quite important because they permit us to generate nanocomposite materials with the highest degree of control of dispersion and hence of mechanical properties.

The effect of the presence of both mono- and multifunctional initiators in the polymerization of styrene was investigated in a solution polymerization of styrene carried out at 100°C using POSS-MAMA-SG1(*b*) as initiator (experiment (5), Table 1). Recall that POSS-MAMA-SG1(*b*) was obtained from the experiment of alkoxyamine **1** with POSS amine in a molar ratio of 12 alkoxyamines **1** for 8 amino groups. Because of the unsuccessful attempt of purification of the resulting product, sample POSS-MAMA-SG1(*b*) contains both mono and multifunctional initiators in a molar proportion of 1:2 with respect to the initiating site. Thus, in the same experiment using POSS-MAMA-SG1(*b*) as initiator, we generate both

star and linear polymers. Similar experiment reported by Gnanou et al. (4), used a mixture that was equimolar in mono and octafunctional initiators with respect to the initiating sites to polymerize styrene. Their objective was to generate both star and linear polymers in the same experiment and by comparing the molar masses of star and linear polymers, they deduced the functionality of star polystyrenes in the condition knowing the real number-average molecular weight of the stars.

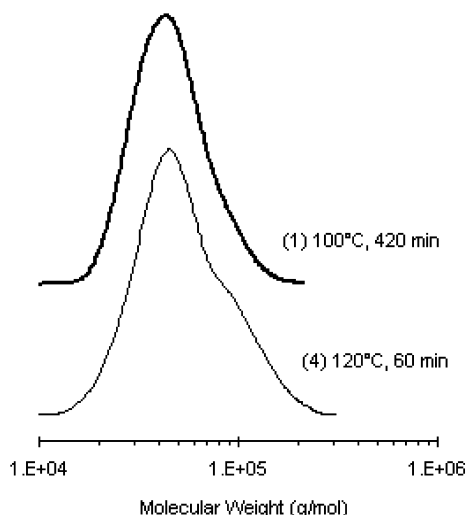


Figure 7. SEC traces of star polymers with similar M_n but obtained under different polymerization conditions. (1) solution polymerization in toluene at 100°C with $M_{n \text{ targeted}} = 110\,000 \text{ g.mol}^{-1}$, (4) solution polymerization in ethylbenzene at 120°C with $M_{n \text{ targeted}} = 110\,000 \text{ g.mol}^{-1}$. For detailed conditions of studies (1) and (4), refer to Table 1.

As we can see, SEC traces shown in Figure 8 exhibited two peaks, the one appearing at lower elution volumes corresponding to the star and the other one to the linear polymer. The SEC elugrams shift steadily to lower elution volumes with increasing conversion as well as for the peaks corresponding to the star than that corresponding to the linear polymers. The multiple Gaussian functions of the chromatography peaks were deconvoluted using Origin software. The molar mass of star and linear polystyrenes, determined by THF SEC according to the relative calibration curve established with linear polystyrene standards, increase linearly with the conversion (Figure 9). The ratios of area under the curve at lower elution volumes to that of the peak at higher elution volumes (RI detector) increase progressively from the value of 0.84 to 1.21 at the beginning to the end of polymerization. This implies that the rates of polymerization

of styrene with respect to mono- and multifunctional initiators were reversed during polymerization. We attributed rather this result by the decrease of the accessibility of stars growing radicals compared to that of linear ones when monomer conversion is increased. Similarly to experiment (1), we also observed a slight shoulder appearing in the high elution volumes of the peaks corresponding to the star polystyrenes (Figure 8) with increasing reaction reaction time. On the other hand, we did not detect any shoulders or even peaks widening for the peaks corresponding to linear polystyrenes. The shoulder observed in the high elution volumes of the peaks corresponding to the star polystyrenes is putatively attributed to the star coupling of the growing radicals due to the proximity of star arms.

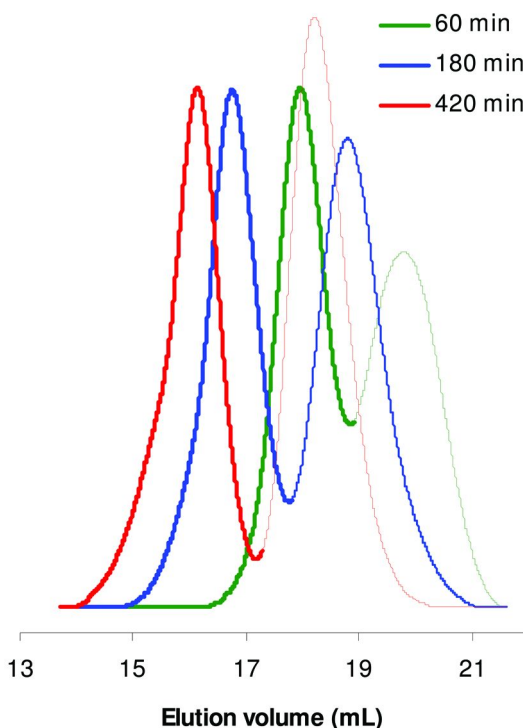


Figure 8. Evolution of the SEC traces (RI detector) at different states of the solution polymerization of styrene using POSS-MAMA-SG1(b) as initiator. Polymerization was carried out in toluene at 100°C with $M_{n \text{ targeted}} = 110\,000 \text{ g.mol}^{-1}$ (study (5), Table 1). Analyzed samples contain a mixture of linear and star polystyrene, peaks in bold lines corresponding to star polystyrene and those in thin lines corresponding to linear one.

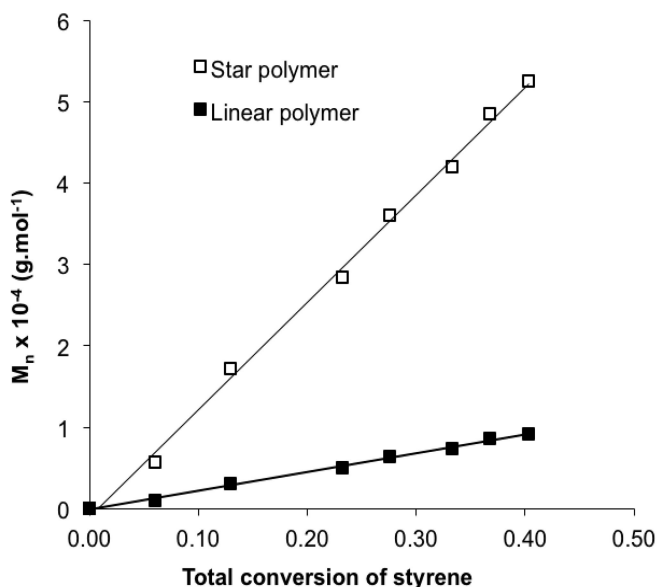


Figure 9. Evolution of M_n (symbols) versus conversion for star and linear PS initiated by POSS-MAMA-SG1(b) in the same solution polymerization of styrene in toluene at 100°C with $M_{n \text{ targeted}} = 110\,000 \text{ g.mol}^{-1}$. Lines are used only to guide the eyes.

Determination of Numbers of Arms

Core destruction has been reported as a useful method to determine the number of branches in star structure (4, 28, 30). The cubes offer a unique opportunity to do this because the PS arms can be disintegrated from the core by cleaving the siloxane bonds of the cubic silsesquioxane with concentrated HF. By comparing the molecular weight of stars before and after core destruction, one can obtain another proof for the star structure. Figure 10 compares the THF SEC traces of the star and cleaved product from experiment (1). Elugram of the cleaved product exhibited a relatively symmetric peak, reporting a dispersity, M_w/M_n of 1.2 and an M_n of 8900 g/mol. The ratio between the molar masses obtained before ($M_n = 45300 \text{ g/mol}$) and after hydrolysis ($M_n = 8900 \text{ g/mol}$) was found to be 5.1 which is slightly below the maximum of 6 arms possible (remind that POSS-MAMA-SG1(a) initiator used in study (1) contained about 5 - 6 initiating sites for each initiator molecule). The problem with this calculation is that star polymers present a lower hydrodynamic volume than a linear polymer with the same molecular weight. This implies that the real number-average molecular weight of the star polymer is higher than 45300 g/mol determined by THF SEC. Besides, once the silsesquioxane is cleaved, the resulted “high” molecular weight product can precipitate as silica gel. If not taken into account, these both factors would contribute to give an incorrect estimation of the number of arms.

Hydrolysis of poorly defined star, product of experiment (4), (in which a shoulder in the high molecular weight region was seen in its SEC trace) also resulted in linear polymers, but the SEC trace, unlike the case of well-defined stars, was not monomodal and presented a shoulder on the high molecular weight region (not shown here). The presence of this shoulder further substantiates the occurrence of star-star coupling during the radical propagation process. Similar results have also been observed by other authors (28, 30) during the preparation of star polymers from POSS-based octafunctional ATRP initiator. In addition, the error in the determination of the number of arms can be affected by star-star coupling. Indeed, when star-star coupling occurs, double or even triple stars could be formed and impedes the propagation of one or two arms, the M_n of coupling arm doubles instantly, thus decreasing the average number of arms.

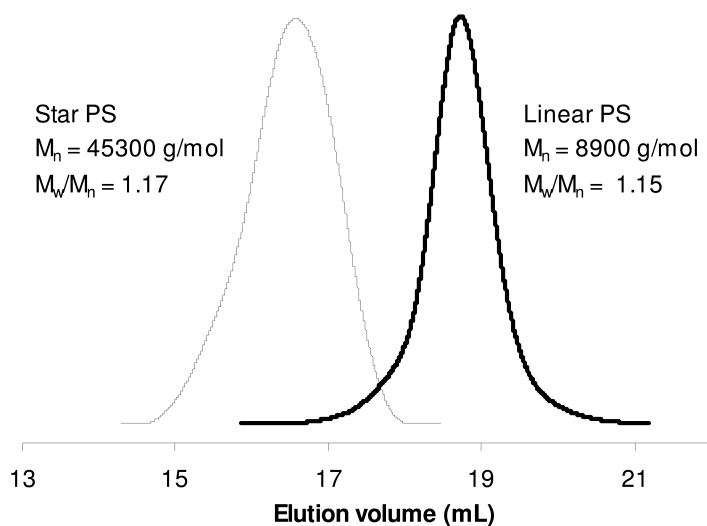


Figure 10. THF SEC traces of one star PS obtained from study (1) $[POSS-MAMA-SG1]/[styrene]_0 = 1 : 1023$; in toluene at 100°C ; and of the cleaved product resulting from reaction of the star with concentrated HF at 40°C .

DSC Studies of Star PS and Their Cleaved Products

Glass transition temperature (T_g) of star-PS1 (well-defined star PS issue from study (1)), star-PS4 (poorly defined star PS issue from study (4)) and their corresponding cleaved products was determined by DSC. Figure 11 shows DSC thermograms of these samples. The data revealed similar T_g values between star-PS1 and star-PS4, they exhibited respectively a T_g of 101 and 99°C. We expected a higher T_g for the poorly defined star PS4 compared to that of the well-defined star PS1 because the inter- and intrastar coupling reactions were more pronounced during the polymerization leading to star PS4 (see Figure 7). When the star coupling reactions occur, the free chain ends of PS arms decrease, which will reduce the chain mobility and thus increase the T_g value. This did not happen in our case because the proportion of chain end decrease resulting from intra or interstar coupling was maybe too low to have a significant effect on the star PS thermal behaviour. Nevertheless, the measured T_g values are largely higher than T_g of a linear PS having the same molecular weight than that of PS arms which means 9000 g/mol. The chemical bonding between PS arms and POSS core that reduces the chains mobility can explain this. This trend was already observed for poly(ethylene oxide) (38), poly(methyl methacrylate) (29) and polystyrene (31) when the latter are attached to the inorganic POSS surface. After etching with HF, T_g values for the cleaved products from well-defined star PS1 and poorly defined star PS4 were determined to be 95 and 89°C, respectively. The treatment with HF resulted in the release of PS arms covalently attached at the POSS surface. Thus, the number of chain ends is doubled; the chains mobility is increased as well as the decrease of overall molecular weight. All of these factors contribute probably to the decrease of T_g for the cleaved products. However, a deeper investigation study is required to understand the underlining mechanism of “confinement” caused by the POSS core on polystyrene segments.

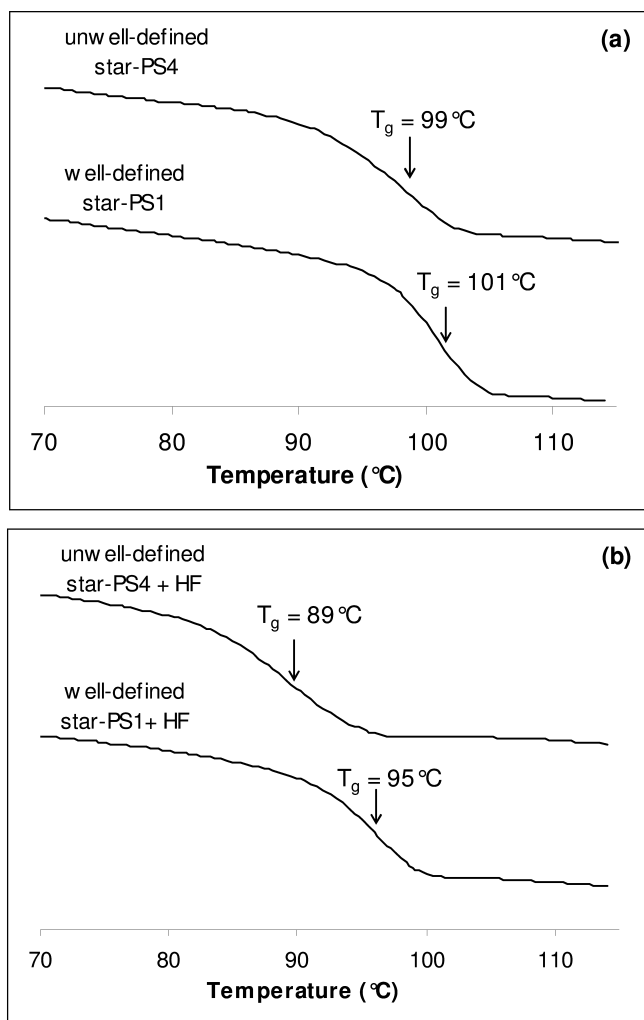


Figure 11. Differential scanning calorimetry thermograms recorded for (a) star polystyrenes and (b) the corresponding cleaved products obtained by treating star PS with HF at 40°C in tetrahydrofuran.

Conclusion

We have successfully synthesized the well-characterized POSS based multifunctional NMP initiator for the first time. The use of the latter in the NMP of styrene allowed producing POSS-core star polystyrenes, which are considered as organic/inorganic hybrid nanocomposites. Well-defined star polystyrenes could be synthesized by maintaining the monomer conversion below 30% and working at a mild temperature about 100°C, beyond which star-star coupling occurs as a result of inevitable termination led to the formation of product with large distribution. By cleaving the core structure with HF solution, the average number of arms was determined to be 5, below the maximum of 6.5 arms possible corresponding to the average number of initiating sites for each initiator molecule. DSC results revealed significantly higher glass transition temperature of POSS-cored star polystyrene as compared with linear PS of comparable molecular weight.

Acknowledgments

This work was financially supported by GENESIS project, University of Provence and CNRS

References

1. Hadjichristidis, N.; Pitsikalis, M.; Pispas, S.; Iatrou, H. *Chem. Rev.* **2001**, *101*, 3747–3792.
2. Charleux, B.; Faust, R. *Adv. Polym. Sci.* **1999**, *142*, 1–69.
3. Hirao, A.; Hayashi, M.; Matsuo, A. *Polymer* **2002**, *43*, 7125–7131.
4. Angot, S.; Murthy, K. S.; Taton, D.; Gnanou, Y. *Macromolecules* **1998**, *31*, 7218–7225.
5. Ueda, J.; Kamigaito, M.; Sawamoto, M. *Macromolecules* **1998**, *31*, 6762–6768.
6. Matyjaszewski, K.; Miller, P. J.; Pyun, J.; Kickelbick, G.; Diamanti, S. *Macromolecules* **1999**, *32*, 6526–6535.
7. Ohno, K.; Wong, B.; Haddleton, D. M. *J. Polym. Sci., Part A: Polym. Chem.* **2001**, *39*, 2206–2214.
8. Stenzel-Rosenbaum, M.; Davis, T. P.; Chen, V.; Fane, A. G. *J. Polym. Sci., Part A: Polym. Chem.* **2001**, *39*, 2777–2783.
9. Zhang, X.; Xia, J.; Matyjaszewski, K. *Macromolecules* **2000**, *33*, 2340–2345.
10. Baek, K. Y.; Kamigaito, M.; Sawamoto, M. *Macromolecules* **2001**, *34*, 215–221.
11. Gao, H.; Matyjaszewski, K. *Macromolecules* **2006**, *39*, 4960–4965.
12. Whittaker, M. R.; Urbani, C. N.; Monteiro, M. J. *J. Am. Chem. Soc.* **2006**, *128*, 11360–11361.
13. Gao, H.; Ohno, S.; Matyjaszewski, K. *J. Am. Chem. Soc.* **2006**, *128*, 15111–15113.
14. Gao, H.; Matyjaszewski, K. *Macromolecules* **2007**, *40*, 399–401.

15. Kakuchi, T.; Narumi, A.; Matsuda, T.; Miura, Y.; Sugimoto, N.; Satoh, T.; Kagas, H. *Macromolecules* **2003**, *36*, 3914–3920.
16. Celik, A.; Kemikli, N.; Ozturk, R.; Muftuoglu, A. E.; Yilmaz, F. *React. Funct. Polym.* **2009**, *69*, 705–713.
17. Kim, K. M.; Ouchi, Y.; Chujo, Y. *Polym. Bull.* **2003**, *49* (5), 341–348.
18. Liu, Y.; Yang, X.; Zhang, W.; Zheng, S. *Polymer* **2006**, *47* (19), 6814–6825.
19. Zhang, C.; Bunning, T. J.; Laine, R. M. *Chem. Mater* **2001**, *13*, 3653–3662.
20. Zheng, L.; Farris, R. J.; Coughlin, E. B. *Macromolecules* **2001**, *34*, 8034–8039.
21. Gonsalves, K. E.; Merhari, L.; Wu, H.; Hu, Y. *Adv. Mater.* **2001**, *13*, 703–714.
22. Lichtenhan, J. D.; Otonari, Y. A.; Carr, M. J. *Macromolecules* **1995**, *28*, 8435–8437.
23. Mather, P. T.; Jeon, H. G.; Romo-Uribe, A.; Haddad, T. S.; Lichtenhan, J. D. *Macromolecules* **1999**, *32*, 1194–1203.
24. Franchini, E.; Galy, J.; Gérard, J. F.; Tabuani, D.; Medici, A. *Polym. Degrad. Stab.* **2009**, *94*, 1728–1736.
25. Pyun, J.; Matyjaszewski, K.; Wu, J.; Kim, G. M.; Chun, S. B.; Mather, P. T. *Polymer* **2003**, *44*, 2739–2750.
26. Xu, H.; Kuo, S. W.; Lee, J. S.; Chang, F. C. *Macromolecules* **2002**, *35*, 8788–8793.
27. Huang, C. F.; Kuo, S. W.; Lin, F. J.; Huang, W. J.; Wang, C. F.; Chen, W. Y.; Chang, F. C. *Macromolecules* **2006**, *39*, 300–308.
28. Costa, R. O. R.; Vasconcelos, W. L.; Tamaki, R.; Laine, R. M. *Macromolecules* **2001**, *34* (16), 5398–5407.
29. Hussain, H.; Mya, K. Y.; Xiao, Y.; He, C. *J. Polym. Sci., Part A: Polym. Chem.* **2008**, *46*, 766–776.
30. Ge, Z.; Zhou, Y.; Liu, H.; Liu, S. *Macromolecules* **2009**, *42* (8), 2903–2910.
31. Lu, C. H.; Wang, J. H.; Chang, F. C.; Kuo, S. W. *Macromol. Chem. Phys.* **2010**, *211*, 1339–1347.
32. Vinas, J.; Chagneux, N.; Gimes, D.; Trimaille, T.; Favier, A.; Bertin, D. *Polymer* **2008**, *49*, 3639–3647.
33. Gravel, M. C.; Zhang, C.; Dinderman, M.; Laine, R. M. *Appl. Organomet. Chem.* **1999**, *13*, 329–336.
34. Naka, K.; Fujita, M.; Tanaka, K.; Chujo, Y. *Langmuir* **2007**, *23*, 9057–9063.
35. Feher, F. J.; Wyndham, K. D. *Chem. Commun.* **1998**, *1998*, 323–324.
36. Matyjaszewski, K.; Miller, P. J.; Fossum, E.; Nakagawa, Y. *Appl. Organomet. Chem.* **1998**, *12*, 667–673.
37. Ananchenko, G. S.; Souaille, M.; Fischer, H.; Le Mercier, C.; Tordo, P. *J. Polym. Sci.: Part A: Polym. Chem.* **2002**, *40* (19), 3264–3283.
38. Maitra, P.; Wunder, L. S. *Chem. Mater.* **2002**, *14*, 4494–4497.